Space Sciences Laboratory
University of California
Berkeley, California 94720

STUDIES OF THE AURORAL SUBSTORM
I. CHARACTERISTICS OF MODULATED ENERGETIC ELECTRON PRECIPITATION OCCURRING DURING AURORAL SUBSTORMS

by

G.K. Parks,* F.V. Coroniti,
R.L. McPherron and K.A. Anderson

Technical Report on

NASA Grant NsG 243-62 and
NSF Grant GP-5583

Space Sciences Laboratory
Series No. 8, Issue No. 45

June 6, 1967

*Now at the School of Physics, University of Minnesota, Minneapolis

ABSTRACT

The temporal, energy and spatial characteristics of energetic auroral zone electron precipitation in the 5-35 second period range are discussed. The electron pulsations of 5-10 second period occur during 0200 to 1000 local time, have a soft energy spectrum with an e-folding energy of about 15 kev, and show spectrum hardening at the peaks. The region over which the electron pulsations are occurring is about 100 to 150 km. The electron pulsations of 20 to 35 second period occur during 1000 to 1500 local time, possess a hard energy spectrum with an e-folding energy of about 30 kev and occasionally show spectral hardening at the peaks. The scale size of these electron pulsations is often 100 to 150 km, but occasionally is greater than 210 km. The electron pulsations and the other forms of energetic electron precipitation that occur in the auroral zone are direct consequences of world-wide disturbance characteristics of auroral substorms.

INTRODUCTION

High altitude balloon measurements of bremsstrahlung x-rays resulting from the precipitation of energetic electrons have shown the presence of diverse temporal structure, from a few milliseconds to hundreds of seconds (for a review paper of auroral zone x-rays, see Brown, 1966; Anderson, 1966).

The purpose of the present article is to discuss in detail the spatial, temporal and energy spectrum characteristics of auroral zone x-rays that exhibit pulsating features in the 5-35 second period range. In paper II (Hereafter and in the two following papers, Parks et al will be referred to as paper I; McPherron, et al as paper II, Coroniti, et al as paper III.) the relationship between energetic electrons and geomagnetic micropulsations is discussed. Recently, Parks, et al (1966) have shown that certain forms of energetic electron precipitation and magnetic micropulsations in the 5-30 second period range were associated with auroral substorms. In paper II, it will be shown that certain forms of energetic electron precipitation are directly related to auroral substorms (Akasofu, 1964). Since local time plays an important role in the ultimate understanding of auroral zone electron precipitation and geomagnetic micropulsation phenomena, we have organized the data in this article in terms of local time.

The various forms of structured energetic electron precipitation phenomena that occur in the auroral zone during geomagnetically disturbed times have been classified into various temporal groups. We review briefly below the various temporal structures in energetic electrons as a function of the local time during which they are most frequently observed.

1. Local Time 2200-0200

Energetic electron precipitation during this time is usually associated with auroral breakup. Until recently, the precipitation is reported to have been intense and featureless over times of a few minutes. However, rocket measurements (Evans, 1967) and balloon-borne measurements at 2 g/cm^2 atmospheric depths (Parks, et al, 1967) indicate the presence of 5-50 millisecond bursts of electrons during auroral breakup. These rapidly varying bursts may be a persistent feature of energetic electron precipitation during these times.

2. Local Time 0200-1000

Brown (1965) and Barcus, et al (1966) have reported numerous observations of x-ray pulsations of 5-10 second periods during these local hours. These x-ray pulsations may be closely related to pulsating auroras (Rosenberg and Bjordal, 1967).

3. Local Time 0600-1400

In this region of local time microbursts are the predominant type of energetic electron precipitation (Anderson, et al, 1966). The characteristic duration of microbursts is 0.1-0.5 seconds. When groups of microbursts occur, the spacing between adjacent microbursts is typically 0.5 seconds (Anderson and Milton, 1964; Parks, 1967). The groups of microbursts are separated by about 10 seconds.

4. Local Time 1000-1500

For the first time, electron pulsations of 20-30 second period have been observed during these local times by the SPARMO group (1966). In this paper data will be presented confirming their observations and detailed properties of these pulsations will be discussed.

5. Local Time 1600-2200

The energetic electron precipitation during these hours generally does not show any significant time variations over several minutes. More data is needed to better our understanding of the properties of this type of electron precipitation.

There are observations of other precipitation forms with temporal variations of about 100 seconds (Evans, 1963; Barcus and Christensen, 1965). However, these have only been observed rarely, and their local time characteristics are not clearly understood.

APPARATUS

The Compton mean scattering length for x-rays of energies 20-150 kev is about 6 g/cm^2. It is important to minimize measurements of scattered photons if accurate information regarding the energy and spatial characteristics of energetic electron precipitation is desired. The data to be presented in this article were obtained from balloons flown at 2-3 g/cm^2 atmospheric depths. A single balloon detector assembly consisted of three NaI(Tl) scintillators, 7.6 cm in diameter and 0.63 cm thick, all of which were pointed in the zenith direction. The detectors were physically collimated with Al-Pb sandwich to give geometrical factors of 9.6 cm^2-ster, 38.6 cm^2-ster and 142 cm^2-ster to view concentric circles of diameter 30 km, 70 km and 210 km at the 100 km stopping heights for electrons. X-rays of energies greater than 20 kev were measured, and energy spectrum information was obtained by use of pulse height discriminators. Also, fast time response analog count-rate meters of the type described by Anderson and Milton (1964) were employed. The true photon rates were obtained by use of in-flight calibrators.

METHOD OF DATA ANALYSES

To obtain the spatial properties of the x-ray pulsations, the analog data corresponding to photons of energies 20-45 kev obtained from the three regions of the sky were compared. The ratios of the x-ray count rate from the different detectors were calculated, and were compared to the theoretically calculated ratios expected at the balloon altitude for an isotropic and uniform x-ray source distribution. The calculation assumed that the bremsstrahlung energy spectrum resulted from an exponential electron energy spectrum. Corrections due to photoelectric and Compton scattering losses and differences in the geometrical factors of the detectors have also been included. It should be noted that with the concentric circular arrangement of the detector system the source distribution is not absolutely known. Thus, our analysis pertains only to changes of a uniform and isotropic x-ray source distribution at the 100 km x-ray production plane. The calculated ratios of the 210 km detector to the 70 km detector is 2.8 and the ratio of the 70 km detector to the 30 km detector is 4.0.

Information on the kinetic energy of the electrons producing the observed x-rays was obtained using thick target bremsstrahlung theory and assuming an exponential electron energy spectrum. After correcting for atmospheric absorption and cosmic ray contributions to the detector count rate, the ratios of the photon count rate in the different energy intervals were compared with the theoretically calculated bremsstrahlung spectra for various electron e-folding energies. The average electron energy obtained in this manner is good to an accuracy of about 30%. This accuracy has already been demonstrated by Hudson, et al (1965). It should be noted that in order to obtain the average energy of the electrons producing the observed bremsstrahlung x-rays the detector energy settings must be taken into consideration. This amounts to adding the energy value of the detector edge setting to the electron e-folding energy. Therefore, the average electron energy causing x-ray pulsations is the e-folding energy plus 20 kev.

RESULTS

Local time 0200 to 1000

During the extended region of local time from 0200 to 1000 the electron precipitation is often modulated with a characteristic period of 5 to 10 seconds. The electrons generally exhibit a soft energy spectrum with a typical e-folding energy of 15 kev. In this section, two representative events will be discussed.

Figure 1 presents the analog x-ray count rate for an event that occurred on September 9, 1966 at 0400 (90° WMT). The electron pulsations occurred on top of a slightly increased x-ray background of 5 photons/cm^2-sec-ster, and have a very regular periodicity and amplitude. Figure 2a shows the results of a power spectrum analysis of this event. The single peak at 5 seconds demonstrates the highly ordered temporal structure of this event. A stretch of data was digitized and is presented along with the ratio of the x-ray count rate in the 20 to 45 kev channel to that in the greater than 45 kev channel is Figure 3. The average electron e-folding energy was about 17 kev. On comparing the temporal changes of the energy spectrum with those of the count rate, it is seen that the peaks of the electron pulsations are generally harder than the background by about 2 kev. It should be pointed out that even though the method of determing the energy spectrum yields values with a possible error of $\pm$ 30%, the changes of the energy spectrum during the electron pulsations are statistically significant. No spatial information for this event is available since only the 70 km detector was flown.

The analog x-ray count rate for the second event which occurred on September 6, 1966 at 0500 (90^{o} WMT) is presented in Figure 4. The background rose to about 50 photons/cm^2-sec-ster in the energy channel 20 to 45 kev for 15 minutes before the start of electron modulation. It is seen that, unlike the previous event, the electron pulsations occurred irregularly, often with a few cycles of modulation separated by unstructured precipitation. The amplitude of the pulsations, however, was roughly constant. Referring to Figure 2b we see that the dominant spectral peaks were 7.0 and 6.3 seconds.

The digitized linear x-ray count rate, the energy ratio of the count rate in the 20 to 45 kev channel to that in the greater than 45 kev channel and the spatial ratio of the count rate in the 210 km detector to that in the 70 km detector is presented in Figure 5. Note that the count rate in the various detectors was high enough so that the counting statistics give only 2 to 3% errors in the ratios. The average e-folding energy of the electrons during this event was 14 kev. On comparing the changes of the energy spectrum with those of the electron pulsations, it is seen that the spectrum always hardens on the rise of the pulsation and softens on the decline. The change in the e-folding energy from the peak to the valley is about 2 kev.

The last part of Figure 5 shows the changes of the ratio of the count rate in the 210 km detector to that in the 70 km detector. Assuming an isotropic flux at the 100 km x-ray production plane, the ratio of the 210 km detector to the 70 km detector on the basis of the theoretical calculation would be 2.8. Comparison of the spatial ratio changes with the x-ray pulsations shows that the ratio decreases during the rise of the pulsation and increases during the decline. At the peaks of the pulsations the ratio is 2.6 whereas at the valley it is 3.4. The fact that the ratio at the valley is higher than the calculated isotropic value of 2.8 is probably due to the pulsation region being centered off axis. The ratio of the count rate in the 70 km detector to that in the 30 km detector (not shown) showed the same systematic changes as the ratio of the 210 km to 70 km. However, the average ratio of 70 km to 30 km was 2.3 whereas the calculated ratio for an isotropic distribution is 4.0. In order to determine whether the detectors and electronics were functioning according to the pre-flight and in-flight calibration, the spatial ratios of the 210 km to 70 km and 70 km to 30 km detectors were checked during the unstructured electron precipitation that occurred just prior to and after this event. In both cases the spatial ratios were those characteristic of an isotropic distribution at the 100 km x-ray production plane.

It would appear, then, that since the 30 km detector was seeing such a high flux this could be interpreted in terms of a scale size of 30 to 50 km in diameter for the region over which the electron pulsations occurred. This result, however, is not unambiguous. For example, a possible interpretation of the high flux in the 30 km detector would be an auroral form of comparable dimension that was centered over the 30 km detector during this event. This could substantially change the flux of the 30 km detector without greatly affecting the 210 or the 70 km detectors. Other spatial distributions that would reproduce the above results are also conceivable. Another possibility is that the region of precipitation could be in systematic motion. A preliminary analysis of the widths and rise times of the pulsations in the three detectors indicates that large scale motions of the precipitation region sweeping across the field of view of the three detectors are not occurring. The temporal resolution of the analysis was sufficient to eliminate the possibility of velocities less than a few hundred kilometers per second.

A further argument against the conclusion that the spatial extent of the pulsating region is 50 km in diameter is that, if it were this small, we would expect to see an occasional pulsation in the 210 km detector and none in the 30 km detector. In all of the electron pulsations analyzed to date, no such case has ever been observed. Our conclusion is that the spatial region of the electron pulsations is probably on the order of 100 to 150 km in extent. We thus tend to confirm an earlier result using two balloons by Barcus, et al (1966) and Brown, et al (1965) that the pulsating region is of the order of 100 km.

Local time 1000 to 1500

The modulated electron precipitation in the region of local time from 1000 to 1500 is characterized by longer periods, 20 to 40 seconds, and by a harder energy spectrum, e-folding energy about 30 kev. The temporal structure is quasi-periodic and even irregular at times, and the amplitude of the pulsations is more variable than in the 5-10 second case. In this section two events will be discussed; the first is a very intense precipitation event, the second is a more typical event which occurred on top of a low background.

The analog x-ray count rate record for the first event which occurred on September 6, 1966 at 1000 (90° WMT) is present in Figure 6. At the start of the event the photon flux was about 400 photons/cm^2-sec-ster in the energy channel 20 to 45 kev. Note that the electron precipitation was unstructured during this most intense part of the event. The photon flux then steadily decreased to about 200 photons/cm^2-sec-ster, and at this point the precipitation became modulated. This event suggests that during very intense electron precipitation, the modulation mechanism is ineffective. Referring to the power spectrum result in Figure 2c, it is seen that there were several broad peaks at 23, 32, 42 and 49 seconds.

A section of digitized linear x-ray count rate, the energy ratio of the count rates in the 20 to 45 kev channel to that in the greater than 45 kev channel, and the spatial ratio of the count rate in the 210 km detector to that in the 70 km detector are presented in Figure 7. The average electron e-folding energy for this event was about 25 kev. The peaks of the electron pulsations are systematically harder than the valleys by 2 to 3 kev. The spatial ratio decreased during the rise of the pulsation, and increased during the decline. The ratio of the count rate in the 70 km detector to that in the 30 km detector was about 5.5, and was constant during a pulsation. This somewhat higher ratio for the 70 km to 30 km and the low ratio 2.6 of the 210 km to 70 km probably means that the pulsation region was centered off axis with respect to the three detectors. As before, the spatial changes imply a scale size for the electron pulsation region of about 100 to 150 km.

Figure 8 presents the analog x-ray count rate for part of an event which occurred on September 8, 1966 at 1300 (90° WMT). The entire event lasted more than one hour although the electron pulsations showed several breaks in continuity during this time. The pulsations occurred on top of a low background of about 20 photons/cm^2-sec-ster in the 20-45 kev channel. Referring to Figure 2d, the power spectrum analysis showed peaks at 20, 25 and 37 seconds. These periods were present throughout the event, thus illustrating the quasi-periodic nature of the longer period electron pulsations. It should also be noted that the amplitude of the electron pulsations was more variable during the event than was the amplitude of the 5-10 second electron pulsations.

The results of the energy spectrum and spatial size analysis showed that the longer period electron pulsations had variable characteristics. In what follows we will present two digitized sections of data that demonstrate this fact. The digitized linear x-ray count rate, the energy ratio, and the spatial ratio are presented in Figure 9 for an early section of the event. The average e-folding energy was 28 kev. There isn't, however, a systematic change of the energy spectrum during an electron pulsation, and both spectral hardening and softening at the peaks occur. The spatial ratio of the count rate in the 210 km detector to the 70 km detector decreases during the rise of the electron pulsation and increases during the decline. The 30 km detector was not used due to its poor counting statistics. For this case, then, the dimension of the precipitating region was about 100 km.

Figure 10 presents the digitized linear x-ray count rate, the energy ratio and the spatial ratio of a section of data from a later part of the event. The energy spectrum is again very hard with an average e-folding energy of 30 kev. In this case, however, the peaks of the electron pulsations are systematically harder than the valleys with a change in e-folding energy of about 5 kev. The spatial ratio, on the other hand, shows no systematic change during an electron pulsation. For this part of the event, then, the scale size of the region of the electron pulsations was greater than 210 km in extent.

DISCUSSION

Before we discuss the significance of the data presented, the salient features of the x-ray pulsations are briefly summarized. In Figure 11, we present a composite of the 5-10 second electron pulsations which typically occur between 0200-1000 local time. The average electron e-folding energy is about 15 kev. The energy spectrum always hardens at the peak of the pulsations with a typical change in the e-folding energy of 2 kev. The temporal structure of these electron pulsations can show a very regular periodicity but can also occur in an irregular manner. Our general impression from analyzing many electron pulsation events is that the pulsations are more periodic when the background of unstructured electron precipitation is low. The amplitude of the electron pulsations for both cases is roughly constant for a time interval long compared to the period of the pulsations. The 5-10 second electron pulsations have a characteristic spatial dimension of about 100-150 km, whereas the unstructured electron precipitation background appears to be isotropic over 210 km. This confirms the previous results of Barcus, et al, (1966).

The longer period pulsations of 20-35 seconds typically occur between 1000 to 1500 local time and exhibit complex energy and spatial characteristics. These electron pulsations are quasi-periodic in nature with a broad range of periods occurring throughout an event. The amplitude is also highly variable. We also note that in the very intense event of September 6, 1966, the modulation of the electron pulsations depended on the total precipitated electron flux, possibly indicating a saturation effect. The average electron energy spectrum of these pulsations is very hard with a typical e-folding energy of 30 kev. Some of the electron pulsations show energy spectral hardening at the peaks; however, occasionally no systematic spectral changes are observed. The results of the spatial analysis indicate that the extent of these electron pulsating regions is often on the order of 100 km and sometimes greater than 210 km. These features have been summarized in the composite diagram shown in Figure 12.

That the various temporal features of auroral zone energetic electron precipitation occur primarily during times when an auroral substorm is in progress will be demonstrated in paper III. Furthermore, it will be shown in paper II that geomagnetic micropulsations and energetic electron precipitation are temporally and causally related. In order to further illustrate the different forms of energetic electron precipitation that occur in the auroral zone during an auroral substorm, we have constructed a schematic figure (Figure 13) showing the results of several hypothetical balloon experiments at various local times. The local time region between 2200-0200 shows the characteristic auroral breakup impulsive electron precipitation of several-minute duration and the rapid 50-millisecond bursts. From 0200-1000 local time the balloon-borne detector would measure 5-10 second electron pulsations. In the overlapping region between 0600 and 1400 local time, microbursts with their characteristic temporal features would be detected. The 20-35 second electron pulsations of the type discussed in this paper would be detected in the local time zone of 1000-1500. In the dusk region, to the best of our knowledge, the electron precipitation would be featureless over several minutes.

ACKNOWLEDGMENTS

We would like to thank Professor R. R. Brown for many helpful discussions. We also wish to thank the various members of the balloon support staff for their generous assistance.

This work was partly supported by the National Aeronautics and Space Administration under grant NsG-243-62. The balloon instruments and balloon flight support were obtained under grant GP-5583 from the National Science Foundation. Administrative and logistic support was provided by the Office of Naval Research Skyhook Program.

REFERENCES

Akasofu, S.-I., The development of the auroral substorm, Planetary Space Sci. 12, 273-282, 1964

Anderson, K.A., Balloon measurements of x-rays in the auroral zone, in Auroral Phenomena, edited by M. Walt, Stanford University Press, Stanford, California 1965

Anderson, K.A., L.M. Chase, H.S. Hudson, M. Lampton, D.W. Milton and G.K. Parks, Balloon and rocket observations of auroral zone microbursts, J. Geophys. Res. 71 (19), 4617-4626, 1966

Anderson, K.A. and D.W. Milton, Balloon observations of x-rays in the auroral zone, 3, High time resolution studies, J. Geophys. Res. 69(21), 4457-4479, 1964

Barcus, J.R., R.R. Brown and T.J. Rosenberg, Spatial and temporal character of fast variations in auroral zone x-rays, J. Geophys. Res. 71(1), 125-141, 1966

Barcus, J.R. and A. Christensen, A 75-second periodicity in auroral zone x-rays, J. Geophys. Res. 70(21), 5455, 1965

Brown, R.R., Electron precipitation in the auroral zone, Space Sci. Rev. 5, 311-387, 1966

Brown, R.R., J.R. Barcus and N.R. Parsons, Balloon observations of auroral zone x-rays in conjugate regions, 2, Microbursts and pulsations, J. Geophys. Res. 70, 2599-2612, 1965

Coroniti, F.V., R.L. McPherron and G.K. Parks, Studies of the auroral substorm, III. Concept of the magnetospheric substorm and its relation to electron precipitation and micropulsations, J. Geophys. Res., this issue

Evans, D.S., A pulsating auroral zone x-ray event in the 100-second period range, J. Geophys. Res. 68, 359-400, 1963

Evans, D.S., On the observation of a 10-cps periodicity in the flux of auroral electrons, Trans. Am. Geophys. Union 48, 72, 1967

Hudson, H.S., G.K. Parks, D.W. Milton and K.A. Anderson, Determinations of the auroral zone x-ray spectrum, J. Geophys. Res. 70(19), 4979-4982, 1965

McPherron, R.L., G.K. Parks, F.V. Coroniti and S.H. Ward, Studies of the auroral substorm, II. Correlated magnetic micropulsations and electron precipitation occurring during auroral substorms, J. Geophys. Res., this issue

Parks, G.K., R.L. McPherron and K.A. Anderson, Relation of 5-40 second period geomagnetic micropulsations and electron precipitation to the auroral substorm, J. Geophys. Res. 71(23), 5743-5745, 1966

Parks, G.K., Spatial characteristics of auroral zone x-ray microbursts, J. Geophys. Res. 72(1), 22, 1967

Parks, G.K., D.W. Milton and K.A. Anderson, Auroral zone x-ray bursts of 5 to 25 millisecond duration, J. Geophys. Res. Letters, to be published 1967

Rosenberg, T.J. and J. Bjordal, Balloon observations of pulsating x-rays and auroras, Trans. Am. Geophys. Union 48, 72, 1967

Simultaneous measurements of auroral x-rays at Kiruna (Sweden) and Ivalo/Sodankylä (Finland) from July to September, 1965, SPARMO Bulletin, No. 2, June, 1966

FIGURE CAPTIONS

Figure 1 - The analog x-ray count rate for a very periodic 5 second electron pulsation event. Note the almost constant amplitude.

Figure 2 - Results of a high resolution power spectrum analysis for the four events discussed in the paper.

Figure 3 - Digitized linear x-ray count rate and the energy ratio for part of the event shown in Figure 1. The average electron e-folding energy was 17 kev. Note that the peak of the electron pulsations are harder than the unstructured precipitation.

Figure 4 - The analog x-ray count rate for a 6 to 10 second period electron pulsation event. Note the rise in the background level before the start of the pulsations and the irregular nature of the modulation.

Figure 5 - Digitized linear x-ray count rate, the energy ratio and spatial ratio for part of the event shown in Figure 4. The average electron e-folding energy was 14 kev, and the peaks are systematically harder than the unstructured precipitation by about 15%. The spatial ratio shows that during an electron pulsation the 70 km detector sees more flux than the 210 km detector indicating a precipitation region of about 100 km in extent.

Figure 6 - Analog x-ray count rate for a 18 to 25 second electron pulsation event. Note the very intense precipitation level at the start of the event and that electron pulsations began after this high level had decreased.

Figure 7 - Digitized linear x-ray count rate, the energy ratio, and spatial ratio for part of the event shown in Figure 6. The average electron e-folding energy was about 25 kev and the peaks of the electron pulsations are harder than the unstructured precipitation by 2 to 3 kev. The spatial ratio shows that during an electron pulsation the 70 km detector sees more flux than the 210 km detector indicating that the precipitation region is about 100 km in extent.

Figure 8 - The analog x-ray count rate for part of a 20-35 second electron pulsation event. The entire event lasted over one hour. Note the quasi-continuous nature of the pulsations.

Figure 9 - Digitized linear x-ray count rate, energy ratio and spatial ratio for part of the electron pulsation event shown in Figure 8. The average electron e-folding energy was 28 kev, but there were no systematic energy spectrum changes during this part of the event. The spatial ratio indicates that the precipitating region for the pulsations was about 100 km in extent.

Figure 10- Digitized linear x-ray count rate energy ratio and spatial ratio for another section of the event shown in Figure 8. The average electron e-folding energy was 30 kev, and the peaks of the electron pulsations are systematically harder than the unstructured precipitation by about 5 kev. The spatial ratio shows no systematic changes during this part of the event implying that region over which the pulsations were occurring was greater than 210 km.

Figure 11 - A composite summary of the temporal, energy, and spatial characteristics of the 5-10 second period electron pulsations typically occurring between 0200-1000 local time.

Figure 12 - A composite summary of the temporal, energy and spatial characteristics of the 20-35 second period electron pulsations typically occurring between 1000-1500 local time.

Figure 13 - A summary of the local time characteristics of the various forms of energetic electron precipitation. Each form occurs at its respective local time during some phase of an auroral substorm.

KEY WORDS

Modulated electron precipitation

x-ray pulsations

Auroral substorm

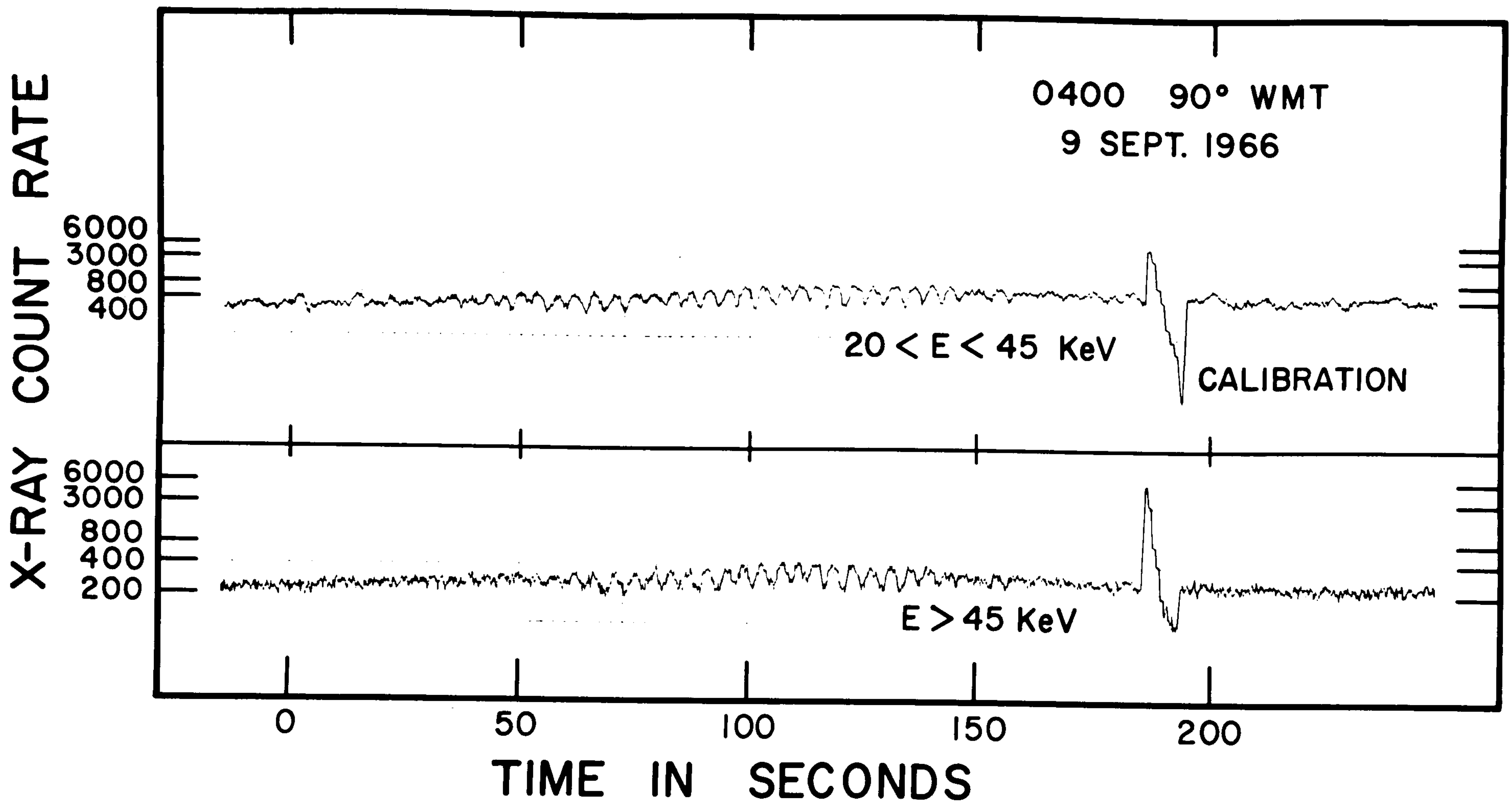
0400 90° WMT
9 SEPT. 1966
X-RAY COUNT RATE
6000
3000
800
400
20 < E < 45 KeV
CALIBRATION
6000
3000
800
400
200
E > 45 KeV
0
50
100
150
200
TIME IN SECONDS

Figure 1

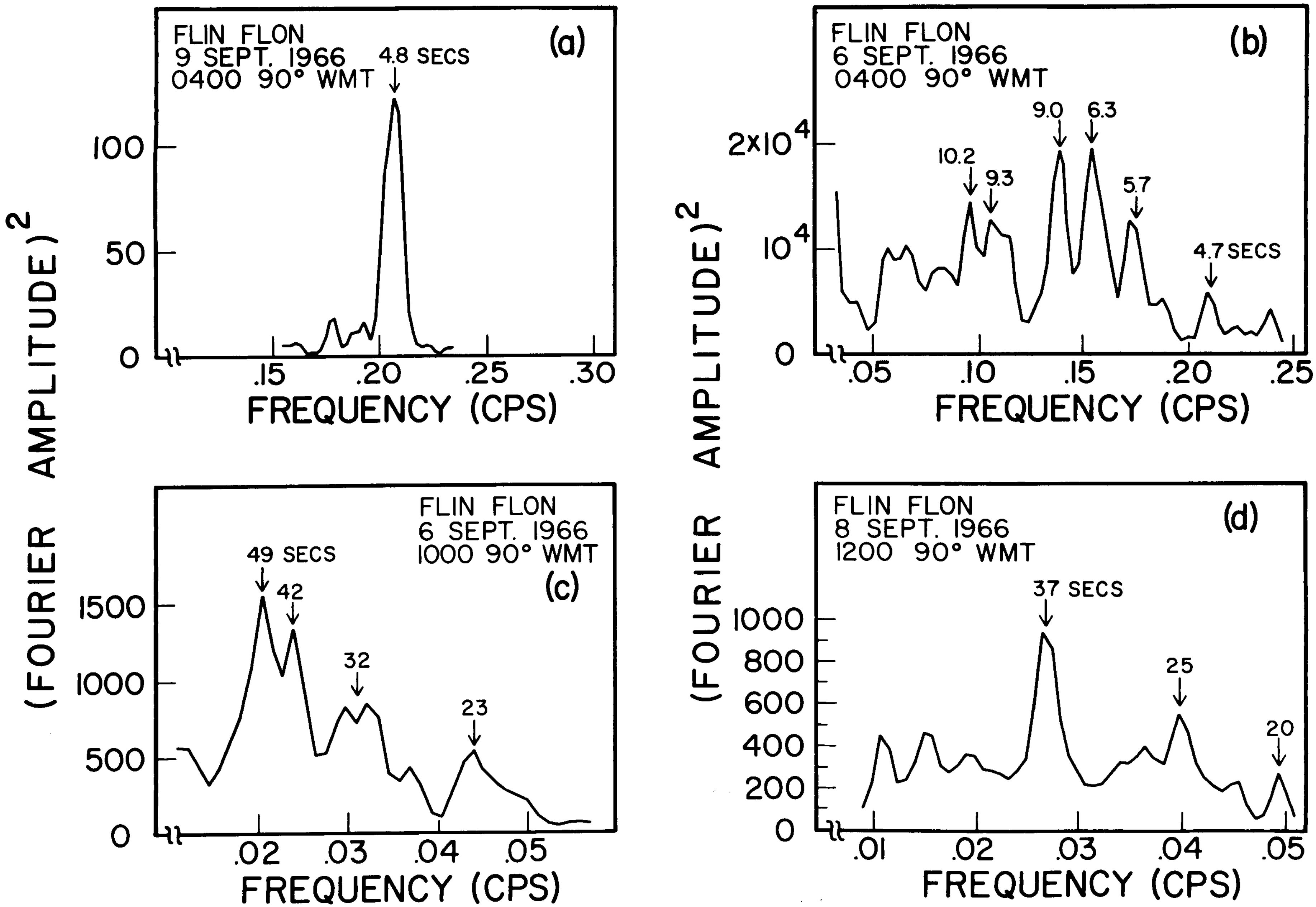
FLIN FLON
9 SEPT. 1966
0400 90° WMT
4.8 SECS
(a)
100
50
0
.15
.20
.25
.30
FREQUENCY (CPS)
FLIN FLON
6 SEPT. 1966
0400 90° WMT
(b)
10.2
9.3
9.0
6.3
5.7
4.7 SECS
2x10^4
10^4
0
.05
.10
.15
.20
.25
FREQUENCY (CPS)
(FOURIER AMPLITUDE)^2
FLIN FLON
6 SEPT. 1966
1000 90° WMT
(c)
49 SECS
42
32
23
1500
1000
500
0
.02
.03
.04
.05
FREQUENCY (CPS)
FLIN FLON
8 SEPT. 1966
1200 90° WMT
(d)
37 SECS
25
20
1000
800
600
400
200
0
.01
.02
.03
.04
.05
FREQUENCY (CPS)
(FOURIER AMPLITUDE)^2

Figure 2

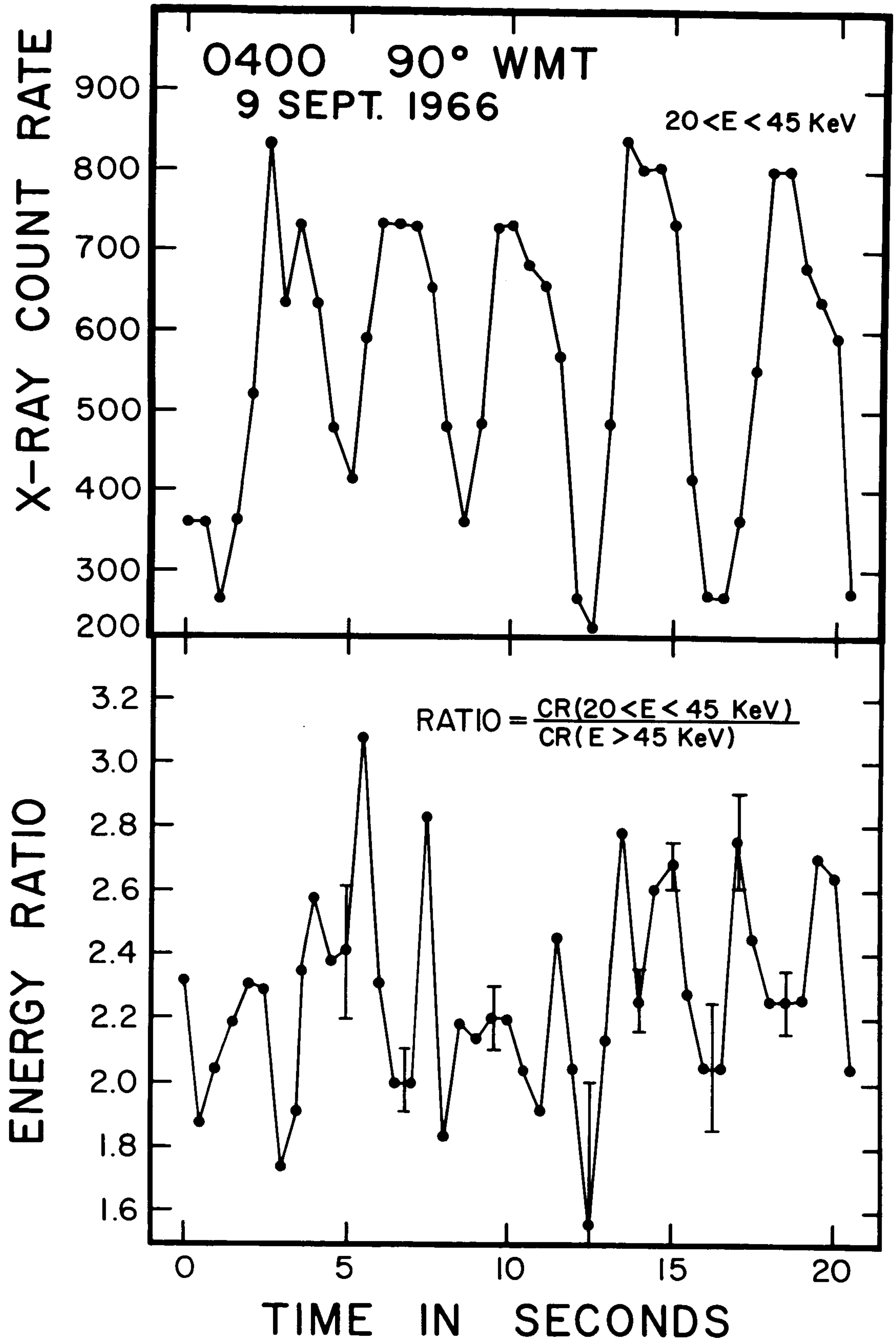

0400 90° WMT
9 SEPT. 1966
20<E<45 KeV
X-RAY COUNT RATE
900
800
700
600
500
400
300
200
RATIO = CR(20<E<45 KeV) / CR(E>45 KeV)
ENERGY RATIO
3.2
3.0
2.8
2.6
2.4
2.2
2.0
1.8
1.6
0
5
10
15
20
TIME IN SECONDS

Figure 3

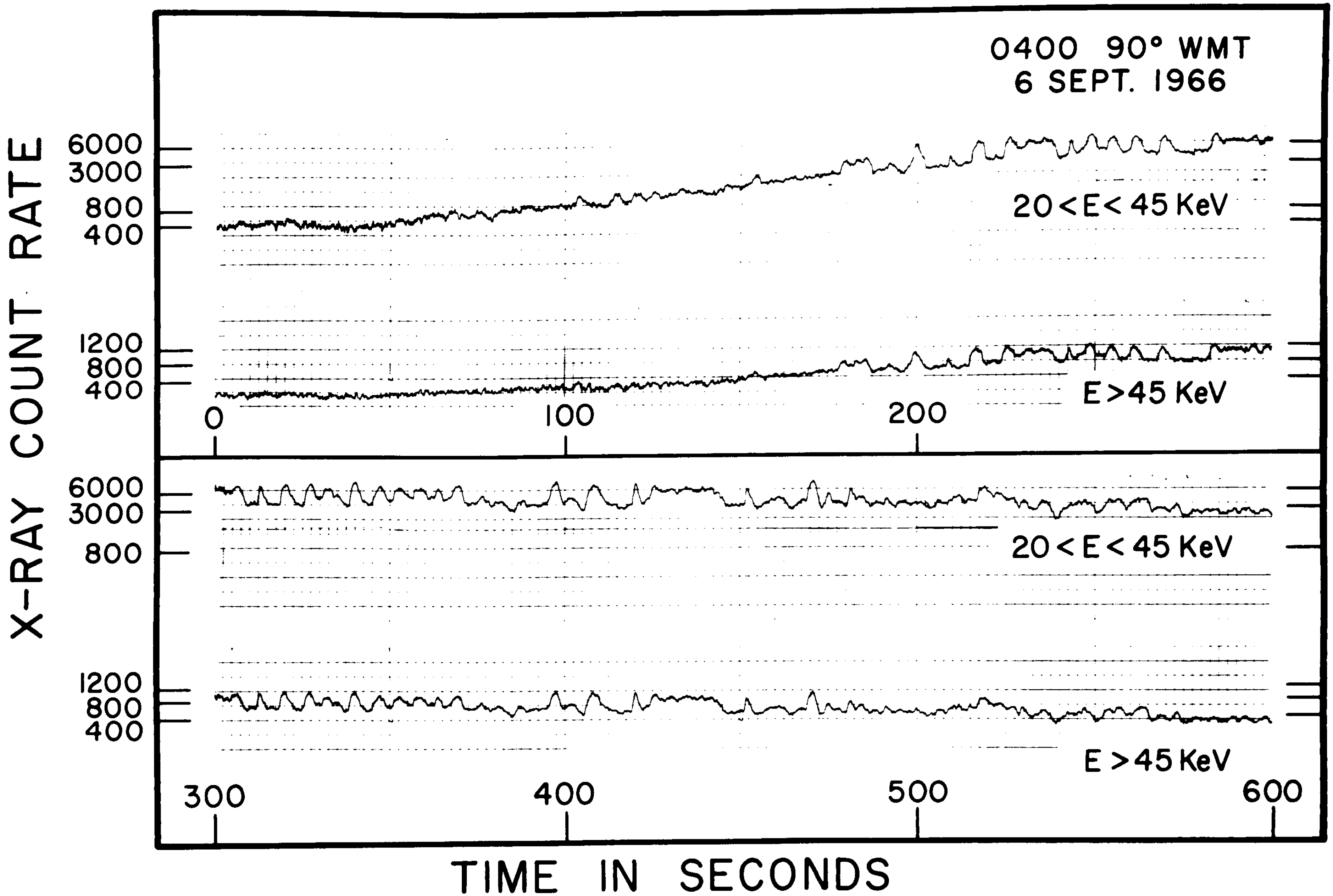
0400 90° WMT
6 SEPT. 1966
X-RAY COUNT RATE
6000
3000
800
400
20 < E < 45 KeV
1200
800
400
E > 45 KeV
0
100
200
6000
3000
800
20 < E < 45 KeV
1200
800
400
E > 45 KeV
300
400
500
600
TIME IN SECONDS

Figure 4

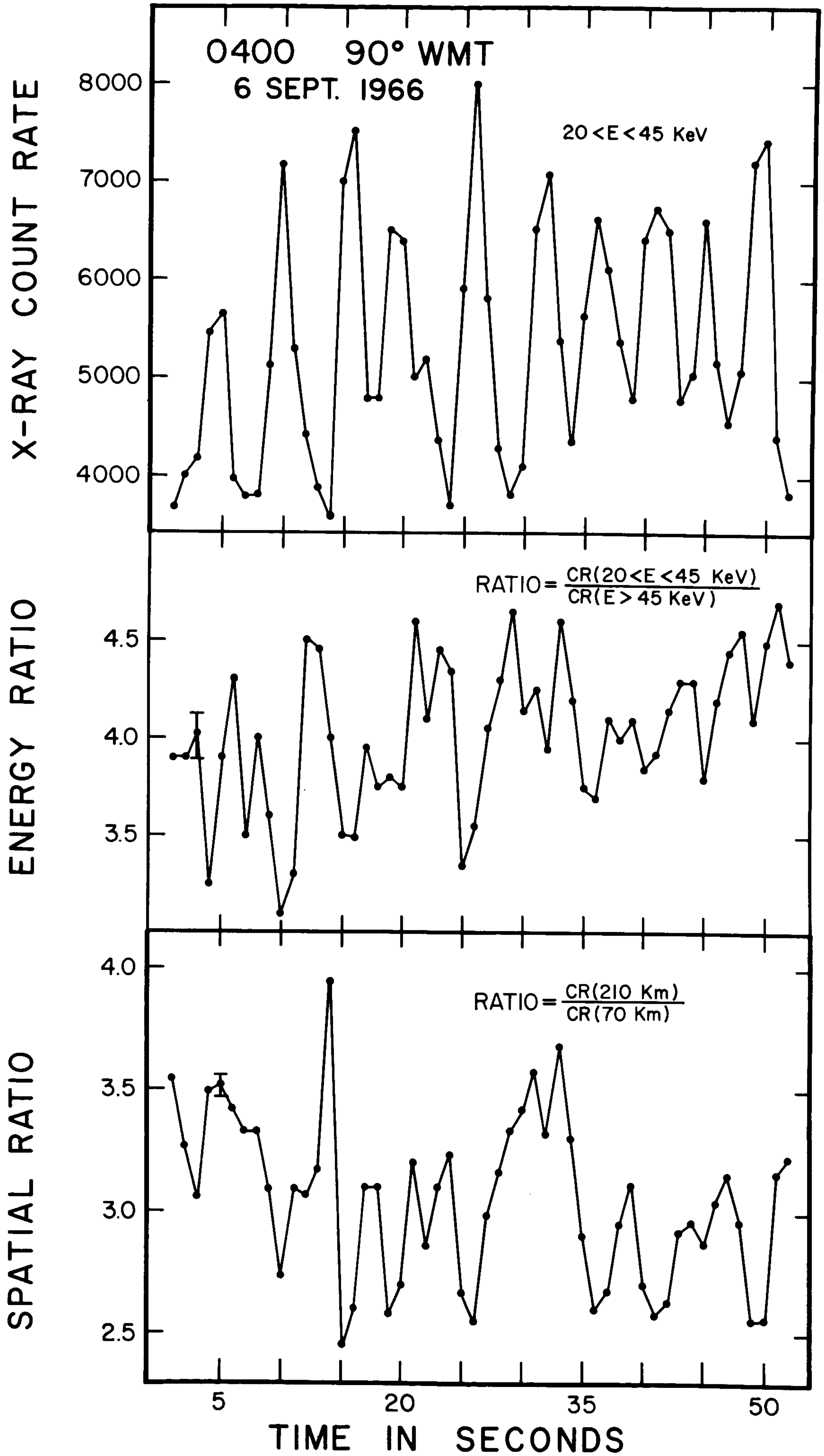

0400 90° WMT
6 SEPT. 1966
20 < E < 45 KeV
X-RAY COUNT RATE
8000
7000
6000
5000
4000
RATIO = CR(20 < E < 45 KeV) / CR(E > 45 KeV)
ENERGY RATIO
4.5
4.0
3.5
RATIO = CR(210 Km) / CR(70 Km)
SPATIAL RATIO
4.0
3.5
3.0
2.5
5
20
35
50
TIME IN SECONDS

Figure 5

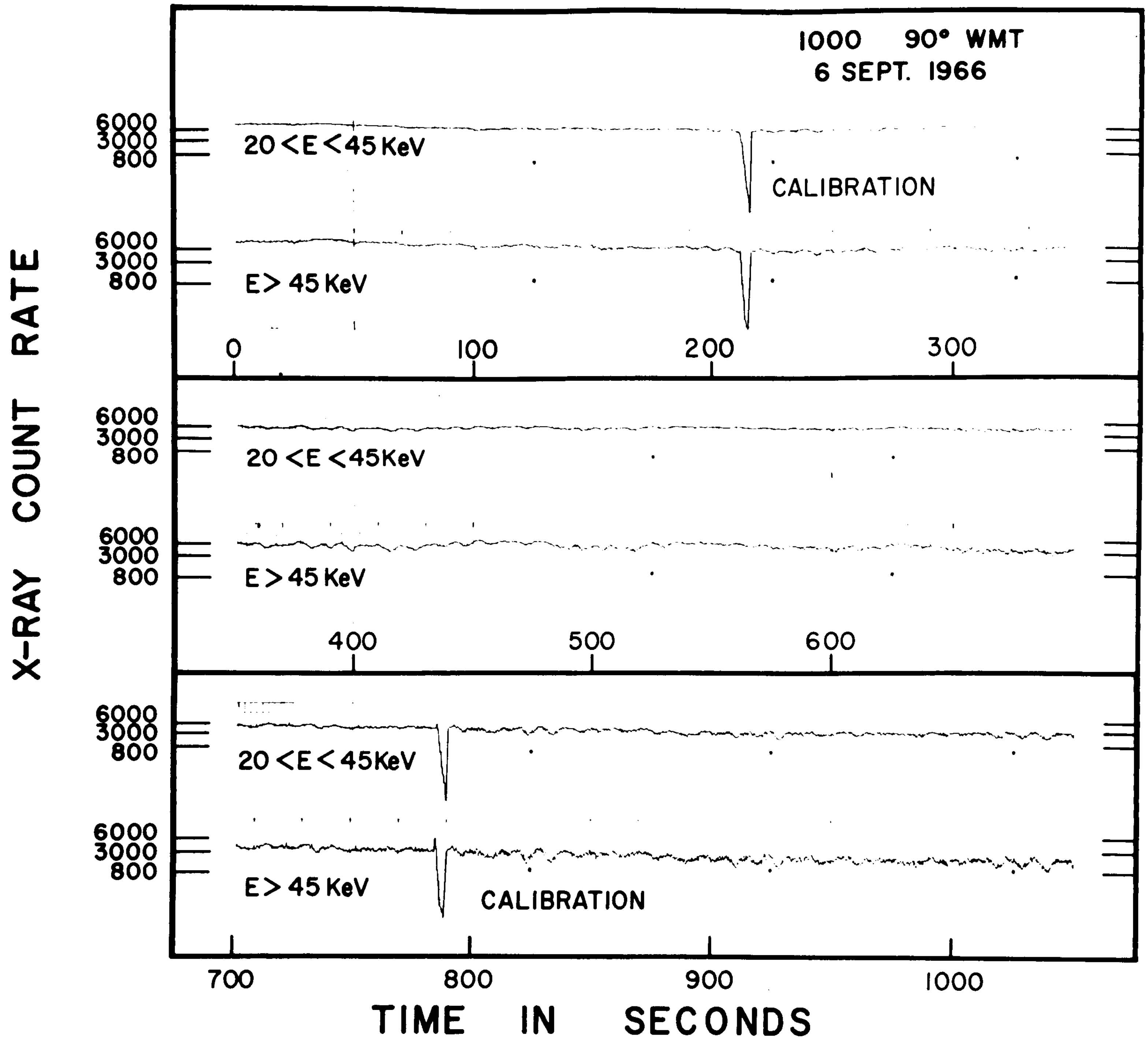
1000 90° WMT
6 SEPT. 1966
X-RAY COUNT RATE
6000
3000
800
20 < E < 45 KeV
E > 45 KeV
CALIBRATION
0
100
200
300
400
500
600
700
800
900
1000
TIME IN SECONDS

Figure 6

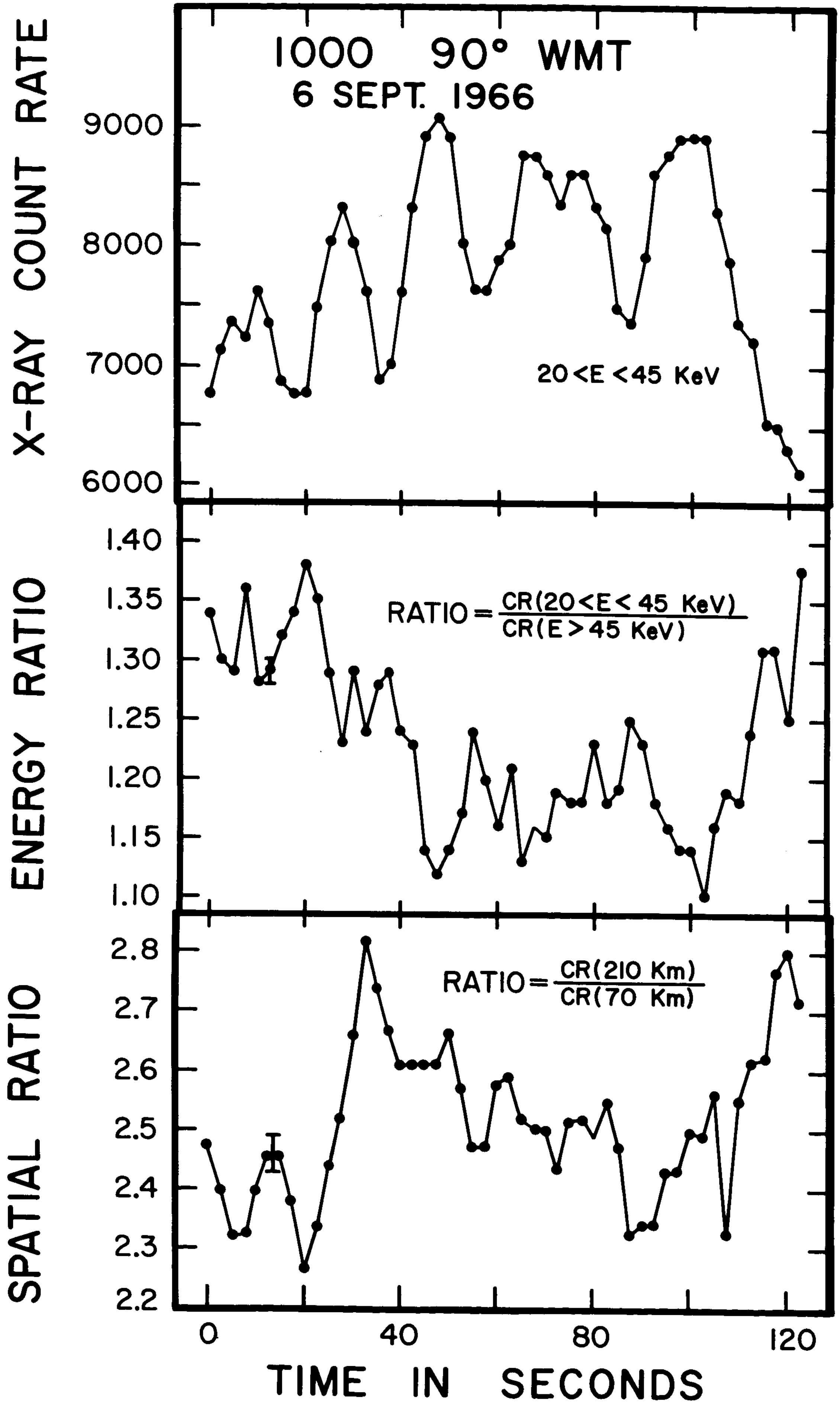

1000 90° WMT
6 SEPT. 1966
X-RAY COUNT RATE
9000
8000
7000
6000
20<E<45 KeV
ENERGY RATIO
1.40
1.35
1.30
1.25
1.20
1.15
1.10
RATIO = CR(20<E<45 KeV) / CR(E>45 KeV)
SPATIAL RATIO
2.8
2.7
2.6
2.5
2.4
2.3
2.2
RATIO = CR(210 Km) / CR(70 Km)
0
40
80
120
TIME IN SECONDS

Figure 7

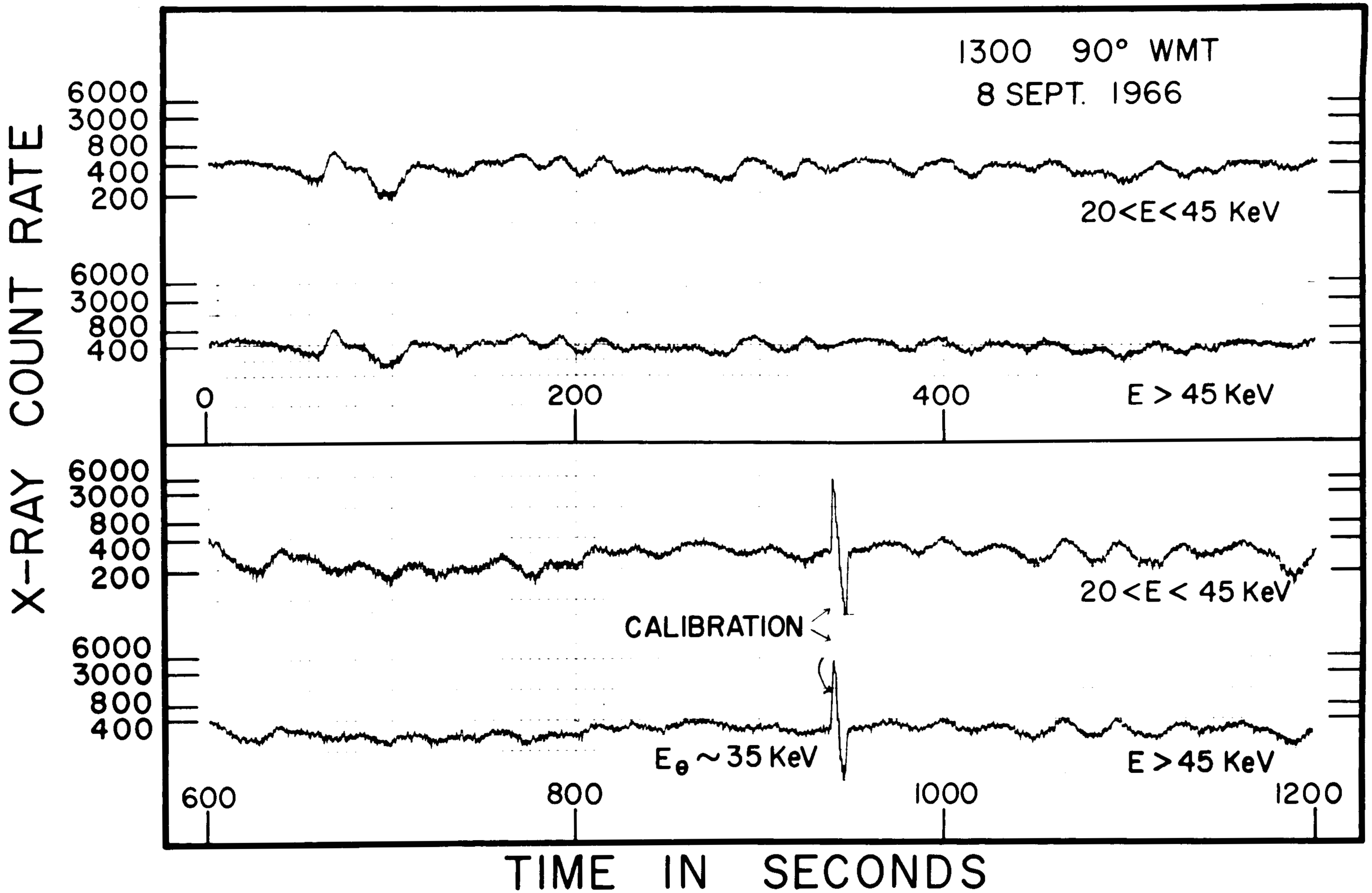
1300 90° WMT
8 SEPT. 1966
X-RAY COUNT RATE
6000
3000
800
400
200
20<E<45 KeV
6000
3000
800
400
E > 45 KeV
0
200
400
6000
3000
800
400
200
20<E< 45 KeV
CALIBRATION
6000
3000
800
400
E_θ ~ 35 KeV
E > 45 KeV
600
800
1000
1200
TIME IN SECONDS

Figure 8

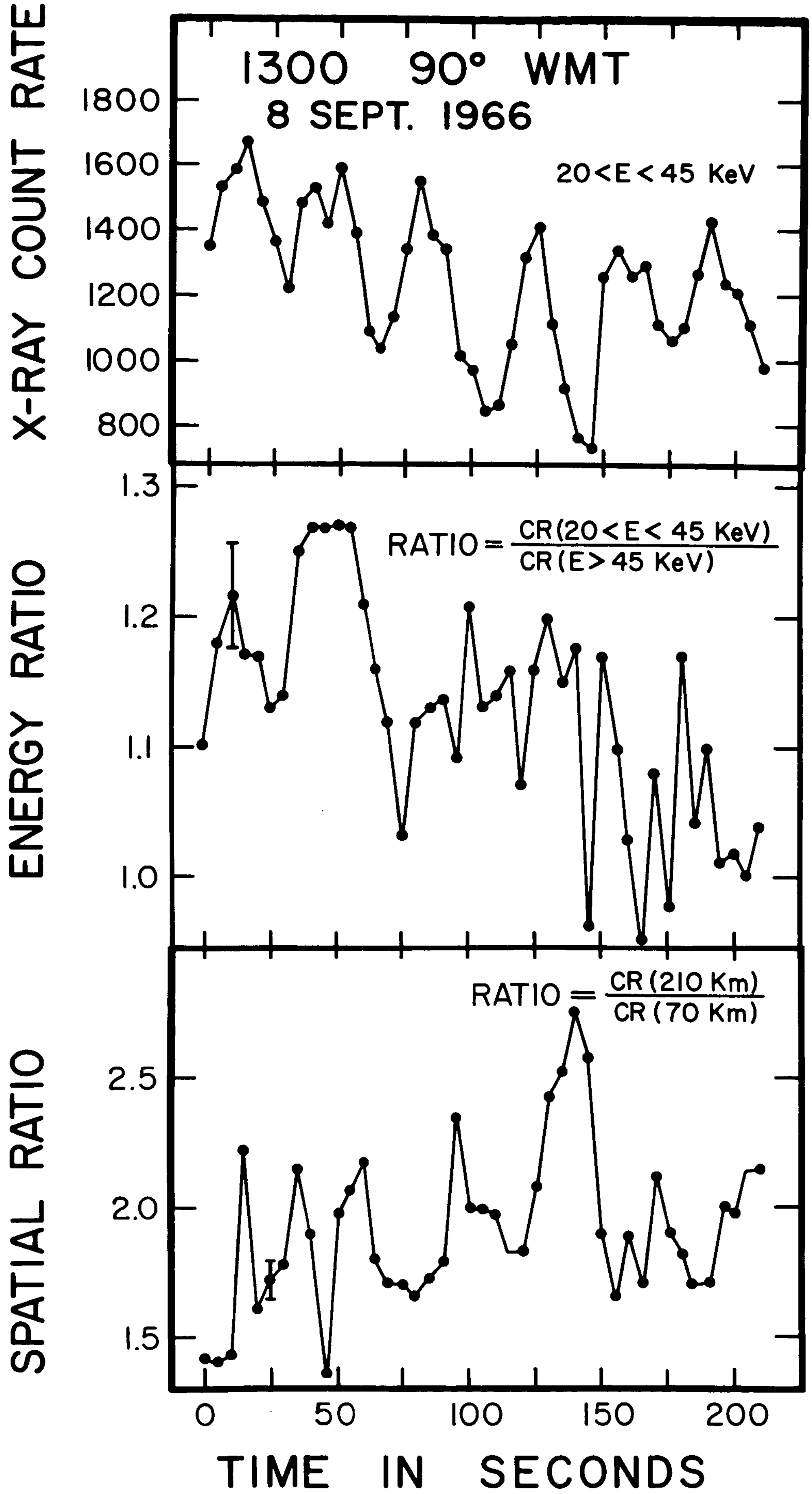
1300 90° WMT
8 SEPT. 1966
20<E<45 KeV
X-RAY COUNT RATE
1800
1600
1400
1200
1000
800
ENERGY RATIO
1.3
1.2
1.1
1.0
RATIO = CR(20<E<45 KeV) / CR(E>45 KeV)
SPATIAL RATIO
2.5
2.0
1.5
RATIO = CR(210 Km) / CR(70 Km)
0
50
100
150
200
TIME IN SECONDS

Figure 9

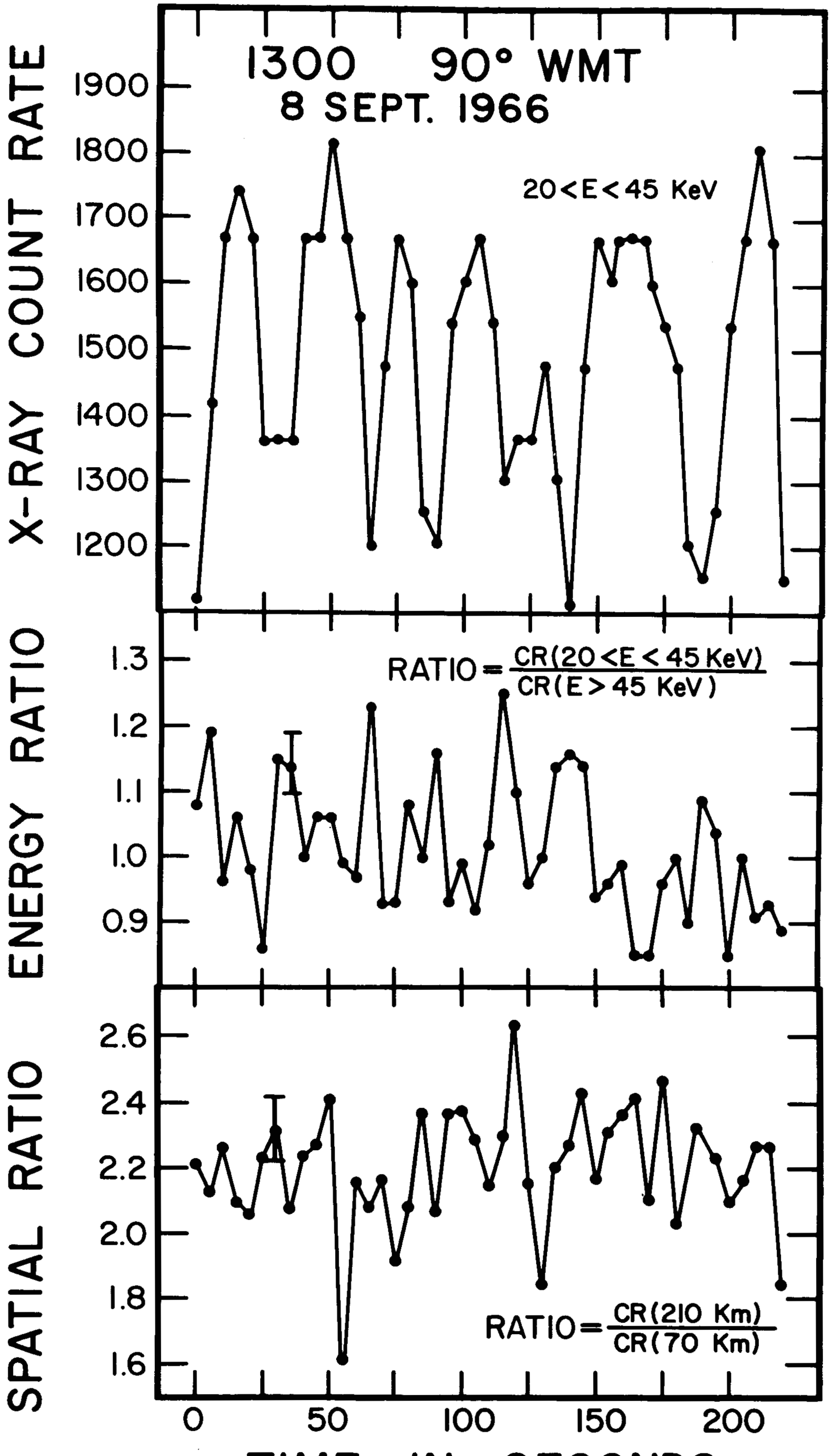

1300 90° WMT
8 SEPT. 1966
X-RAY COUNT RATE
1900
1800
1700
1600
1500
1400
1300
1200
20<E<45 KeV
ENERGY RATIO
1.3
1.2
1.1
1.0
0.9
RATIO = CR(20<E<45 KeV) / CR(E>45 KeV)
SPATIAL RATIO
2.6
2.4
2.2
2.0
1.8
1.6
RATIO = CR(210 Km) / CR(70 Km)
0
50
100
150
200
TIME IN SECONDS

Figure 10

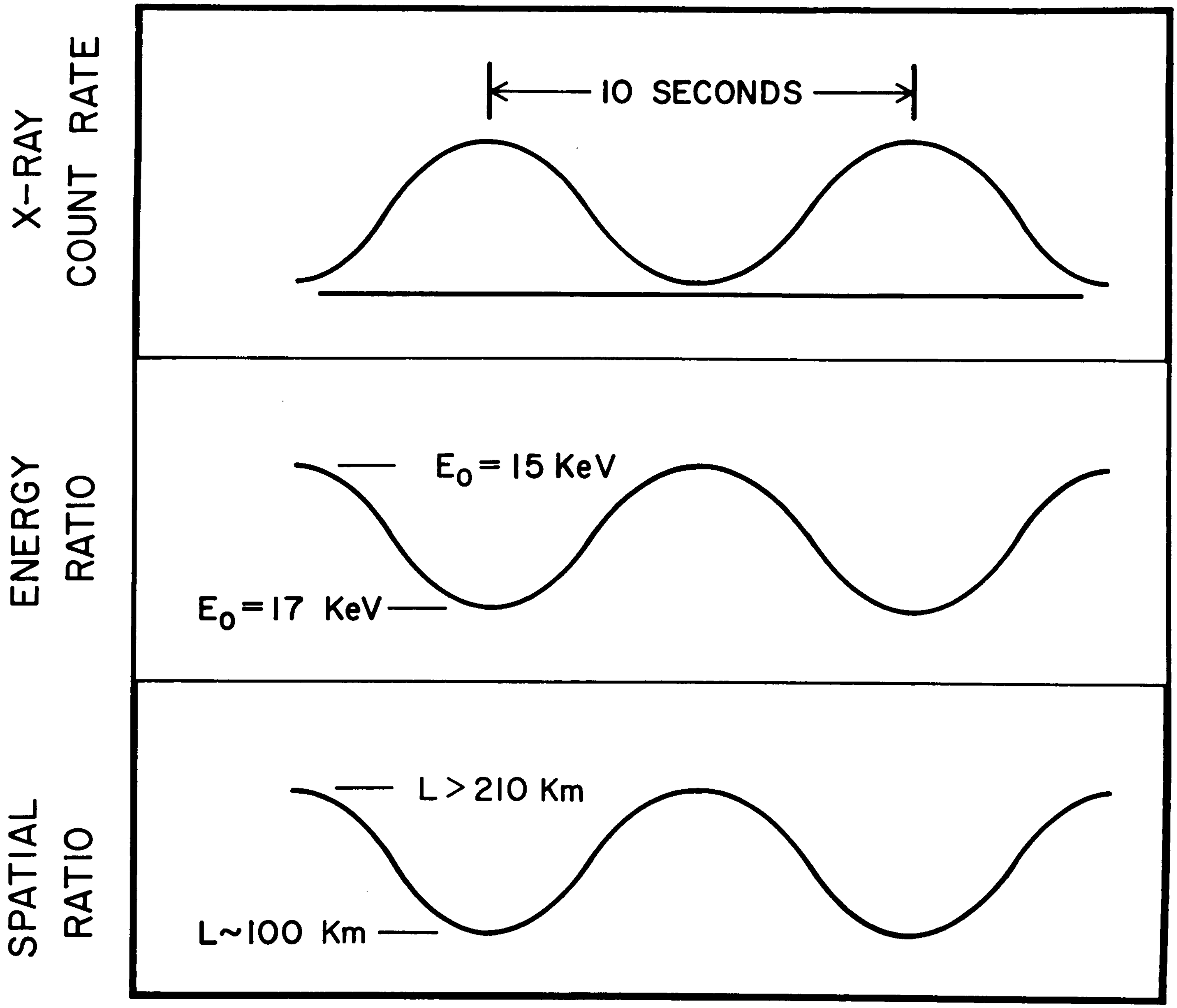
X-RAY
COUNT RATE
10 SECONDS
ENERGY
RATIO
$E_0 = 15$ KeV
$E_0 = 17$ KeV
SPATIAL
RATIO
L > 210 Km
L~100 Km

Figure 11

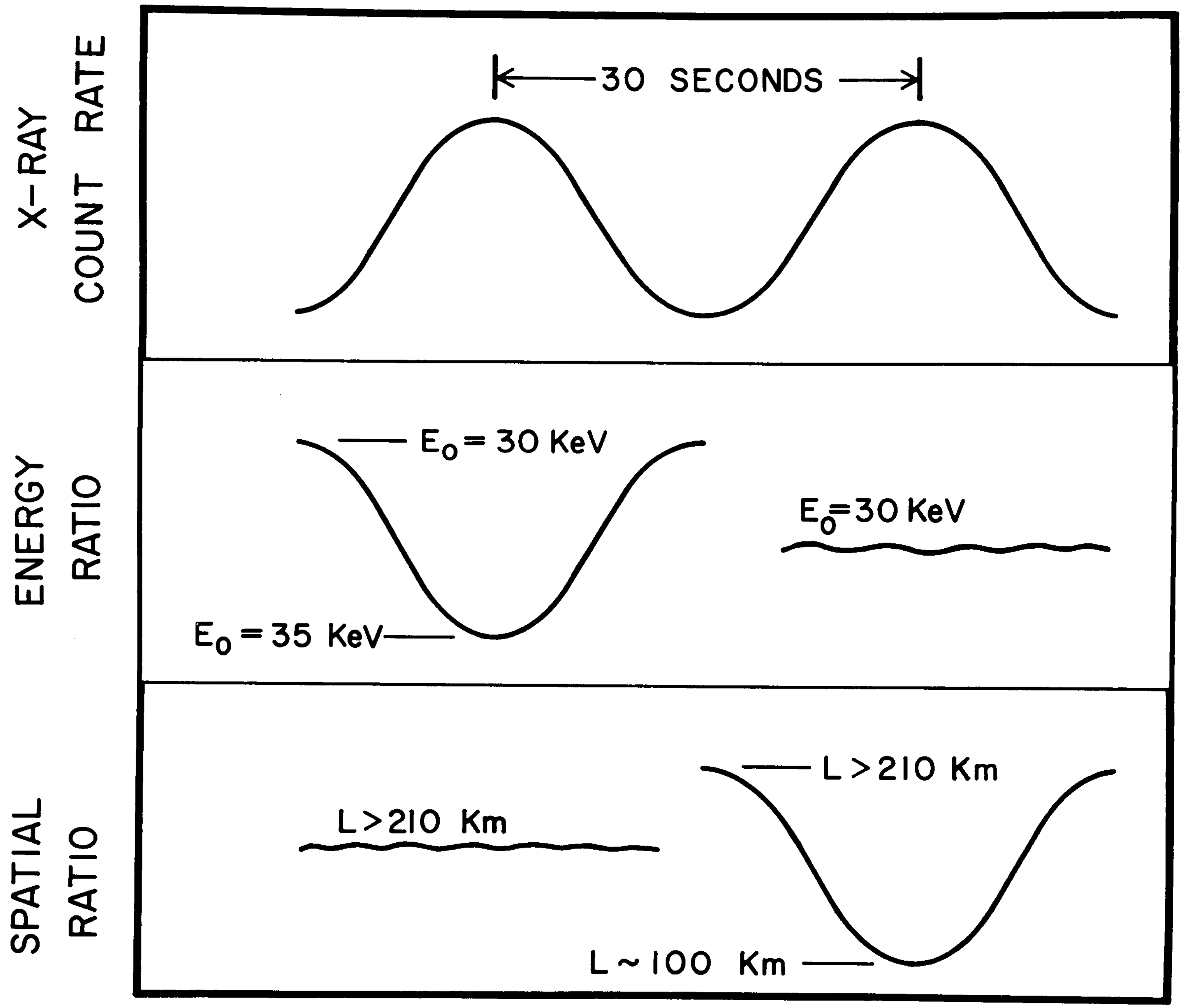
X-RAY
COUNT RATE
30 SECONDS
ENERGY
RATIO
$E_o = 30$ KeV
$E_o = 35$ KeV
$E_o = 30$ KeV
SPATIAL
RATIO
L>210 Km
L>210 Km
L~100 Km

Figure 12

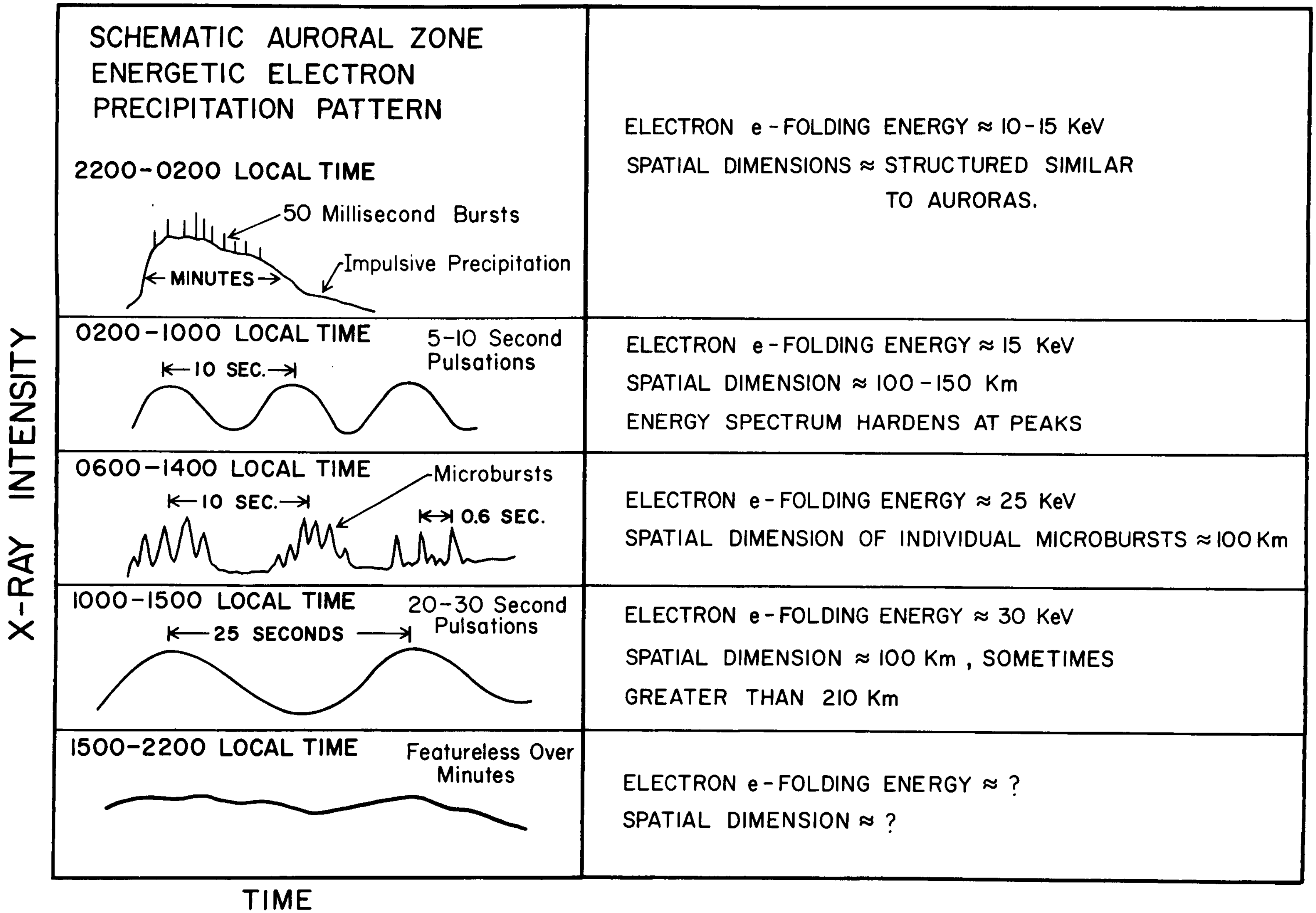
SCHEMATIC AURORAL ZONE
ENERGETIC ELECTRON
PRECIPITATION PATTERN
2200-0200 LOCAL TIME
50 Millisecond Bursts
Impulsive Precipitation
MINUTES
ELECTRON e-FOLDING ENERGY ≈ 10-15 KeV
SPATIAL DIMENSIONS ≈ STRUCTURED SIMILAR
TO AURORAS.
0200-1000 LOCAL TIME
5-10 Second
Pulsations
10 SEC.
ELECTRON e-FOLDING ENERGY ≈ 15 KeV
SPATIAL DIMENSION ≈ 100-150 Km
ENERGY SPECTRUM HARDENS AT PEAKS
0600-1400 LOCAL TIME
Microbursts
10 SEC.
0.6 SEC.
ELECTRON e-FOLDING ENERGY ≈ 25 KeV
SPATIAL DIMENSION OF INDIVIDUAL MICROBURSTS ≈ 100 Km
1000-1500 LOCAL TIME
20-30 Second
Pulsations
25 SECONDS
ELECTRON e-FOLDING ENERGY ≈ 30 KeV
SPATIAL DIMENSION ≈ 100 Km, SOMETIMES
GREATER THAN 210 Km
1500-2200 LOCAL TIME
Featureless Over
Minutes
ELECTRON e-FOLDING ENERGY ≈ ?
SPATIAL DIMENSION ≈ ?
X-RAY INTENSITY
TIME

Figure 13